OPEN ACCESS
IOP Publishing
Plasma Physics and Controlled Fusion
Plasma Phys. Control. Fusion **60** (2018) 055006 (13pp)
https://doi.org/10.1088/1361-6587/aab25a

A forward model for the helium plume effect and the interpretation of helium charge exchange measurements at ASDEX Upgrade

A Kappatou[1], R M McDermott[1], T Pütterich[1], R Dux[1], B Geiger[1], R J E Jaspers[2], A J H Donné[2,3], E Viezzer[4], M Cavedon[1] and the ASDEX Upgrade Team

[1] Max-Planck-Institut für Plasmaphysik, D-85748 Garching, Germany
[2] Science and Technology of Nuclear Fusion, Eindhoven University of Technology, 5612 AZ Eindhoven, The Netherlands
[3] EUROfusion Programme Management Unit, D-85748 Garching, Germany
[4] Department of Atomic, Molecular and Nuclear Physics, University of Seville, E-41012 Seville, Spain

E-mail: Athina.Kappatou@ipp.mpg.de

Received 5 December 2017, revised 16 February 2018
Accepted for publication 26 February 2018
Published 23 March 2018

Abstract

The analysis of the charge exchange measurements of helium is hindered by an additional emission contributing to the spectra, the helium 'plume' emission (Fonck *et al* 1984 *Phys. Rev.* A **29** 3288), which complicates the interpretation of the measurements. The plume emission is indistinguishable from the active charge exchange signal when standard analysis of the spectra is applied and its intensity is of comparable magnitude for ASDEX Upgrade conditions, leading to a significant overestimation of the He^{2+} densities if not properly treated. Furthermore, the spectral line shape of the plume emission is non-Gaussian and leads to wrong ion temperature and flow measurements when not taken into account. A kinetic model for the helium plume emission has been developed for ASDEX Upgrade. The model is benchmarked against experimental measurements and is shown to capture the underlying physics mechanisms of the plume effect, as it can reproduce the experimental spectra and provides consistent values for the ion temperature, plasma rotation, and He^{2+} density.

Keywords: helium density, helium plume emission, charge exchange recombination spectroscopy, ASDEX Upgrade

(Some figures may appear in colour only in the online journal)

1. Introduction

The successful operation of ITER [1] and other future fusion devices relies strongly on the understanding of helium transport in the plasma as accumulation of helium 'ash' in the plasma core would dilute the fusion fuel [2]. Significant efforts have been made to understand the behaviour of the helium density profile in fusion plasmas, of both experimental and theoretical nature [3, 4]. Helium in the plasma can be diagnosed by means of active charge exchange recombination spectroscopy on a neutral beam (or other neutral source), a powerful diagnostic technique that provides spatially and temporally resolved measurements of ion temperature, plasma rotation and impurity density in the plasma. At ASDEX Upgrade [5], the helium charge exchange measurements are based, as is most commonly done, on the HeII line at 468.571 nm (transition $n = 4 - 3$), which can be performed with standard optical instruments that operate in the visible range. However, helium charge exchange measurements are hindered by the so-called 'plume' effect [6], the additional

emission due to electron collisional excitation of the He^+ ions produced by charge exchange reactions along the neutral beam, which drift away from their birth location. This feature has a strong impact on the measurement and cannot be distinguished via a standard analysis from the prompt charge exchange signal or avoided using techniques such as beam modulation. For accurate helium density profile measurements, and subsequently accurate helium transport analyses, the helium plume effect and the emission contributed to the measured spectra have to be considered for each individual line-of-sight (LOS) and diagnostic configuration and forward models for its interpretation are required.

In the past, a number of studies have been conducted in order to understand the helium plume effect and to model the helium plume emission. The helium plume effect was first described and named by Fonck *et al* in [6]. In that publication the helium plume effect is identified as a significant disturbance to the helium charge exchange spectra and a simplified model for the evaluation of the plume emission is proposed. The dependence of the plume emission on parameters such as the diagnostic observation geometry and the beam energy is described. It is also noted that no accurate toroidal rotation profiles can be obtained from the helium charge exchange spectra if the plume effect is not taken into account. Gerstel *et al* attempted in [7], to calculate both the plume from the thermal helium content in the plasma, but also the helium beam 'plume', as part of the analysis of helium beams. Here a Monte Carlo approach was employed for solving the transport equation of the hydrogenic plume ions. Nevertheless, the helium plume emission is not shown to be taken into account in the fitted helium spectra. In [8], it is mentioned that the plume emission calculated from the model in [7] is overestimated by a factor of 3 in intensity. The helium plume emission was also studied at DIII-D [3] following a method similar to the one described in [6] as well as considering a Maxwellian distribution to describe the plume ions. The plume emission corrections were found to be important only in terms of magnitude, but not significant in terms of profile shapes. A further effort to model the helium plume can be found in [9], where the method developed in [6] is also followed.

These previous investigations and models of the helium plume emission have resulted in significant progress in understanding the helium plume emission and its impact on the measurement. However, no model has been benchmarked against experimental data or has been shown to accurately reproduce the experimental spectra. In this work, a forward model following a Monte Carlo approach is presented for the charge exchange spectroscopy diagnostic at ASDEX Upgrade. The benchmarking of the model against experimental data, as well as its ability to reproduce the measured helium charge exchange spectra are described.

The helium content in the plasma is measured routinely at ASDEX Upgrade utilising a high étendue spectrometer designed for core charge exchange measurements in ITER [10]. This instrument measures three wavelength ranges simultaneously, namely the carbon, helium and D_α (beam emission) spectra. In the helium spectra obtained at ASDEX Upgrade, the existence of the helium plume emission can be identified experimentally in two ways.

First, a comparison of the ion temperature (T_i) and toroidal rotation (v_ϕ) profiles derived from the helium charge exchange measurements and those derived from measurements on boron or carbon, which are routinely measured on ASDEX Upgrade, reveals a disagreement between the two sets of measurements. As will be explained in more detail in this work, such a disagreement is due to the plume emission, if there is a significant plume contribution in the measured spectra. Second, the helium density profiles derived from different diagnostic observation geometries (e.g. poloidal and toroidal LOS) do not agree. This too is expected if there is significant plume contribution to the spectra, as will be discussed in section 3.2. Both of these indications for the plume are observed at ASDEX Upgrade and will be explained by means of the helium plume model presented here.

In section 2 the helium plume effect is presented and the forward model implemented for ASDEX Upgrade is described in section 3. In section 4, the helium plume model is benchmarked against experimental data. Final comments are given in the last section.

2. The helium plume emission

The following description of the plume applies to magnetically confined hydrogen or deuterium plasmas into which a hydrogen or deuterium neutral beam is injected for heating or diagnostic purposes and in which, we assume, there is a trace population of helium ions. The standard ASDEX Upgrade operating conditions of deuterium plasmas and deuterium neutral beams will be used for the discussion.

Following the charge exchange reactions between fully ionised helium ions and deuterium neutrals, a population of He^+ ions is born in the neutral beam volume:

$$He^{2+} + D^0 \rightarrow He^+ + D^+. \quad (1)$$

These He^+ ions are eventually reionised to fully stripped helium mostly due to electron impact. However, there is a finite time before the reionisation takes place, equal to the ionisation time $\tau_{ion} = (n_e \cdot q^e_{ion}(T_e, n_e))^{-1}$, where q^e_{ion} is the electron impact ionisation rate and n_e and T_e are the plasma electron density and temperature, respectively. During this time, the He^+ ions can travel along the magnetic field lines away from their birth locations. Along the way, there is a high probability that they are excited by electron and ion impact. If they are excited back up to the $n = 4$ state, then they can decay into the $n = 3$ and emit additional photons at the same wavelength as the active charge exchange signal (HeII line, $n = 4 - 3$), causing an additional contribution to the measured signal. This is the so-called helium plume emission [6]. The helium plume signal is superimposed on and of comparable magnitude to the active charge exchange (prompt) signal. As such, it disturbs the measurements and leads to an

overestimation of the He^{2+} density as well as erroneous ion temperature and velocity measurements.

The prompt charge exchange emission corresponding to each diagnostic LOS depends on the local He^{2+} density, as well as the local neutral beam density, and the relevant charge exchange cross-sections. The photon radiance Φ_{CX} due to the charge exchange reactions can be written as:

$$\Phi_{CX} = \frac{1}{4\pi}\sum_{i=1}^{4}\sum_{n=1}^{2}\int_{LOS}\langle\sigma_{CX}(\upsilon_{col})\cdot\upsilon_{col}\rangle^{i,n}n_b^{i,n}(l)n_{He^{2+}}(l)\mathrm{d}l, \tag{2}$$

where l is the coordinate along the LOS, $\langle\sigma_{CX}(\upsilon_{col})\cdot\upsilon_{col}\rangle^{i,n}$ is the effective rate coefficient for a charge exchange reaction and subsequent emission of a photon for the observed transition, $n_b(l)$ is the local neutral beam density, $n_{He^{2+}}(l)$ the local He^{2+} density, and the integration is over the intersection of the LOS through the neutral beam. The index i indicates the different velocity components of the neutral beam ($i = 1$–3) including the halo ($i = 4$) and the index n is the principle quantum number. The halo neutral cloud is broader than the neutral beam and its density can be comparable to or larger than the neutral beam density. Only charge exchange reactions with neutrals in the $n = 1$ and $n = 2$ have been taken into account in this work.

On the other hand, the total radiance of the helium plume emission observed is given by:

$$\Phi_{Plume} = \frac{1}{4\pi}\int_{LOS} n_{He^{+}}n_e Q_{exc}^{e}\mathrm{d}l, \tag{3}$$

where Q_{exc}^{e} is the effective electron impact excitation coefficient, as obtained from a collisional-radiative model [11]. For typical ASDEX Upgrade plasmas, only electron impact excitation is relevant. However, at higher temperatures, ion impact excitation can become important. $n_{He^{+}}$ depends on the source of He^{+} ions, i.e. on all the charge exchange reactions that lead to the production of He^{+} ions, as well as the ionisation time.

Calculation of the helium plume emission, therefore, requires knowledge of the He^{+} density along the LOS of the diagnostic. To obtain this information, the He^{+} born in the beam volume due to charge exchange reactions must be followed along the magnetic field lines and the density of the He^{+} ions at the intersection points of the magnetic field lines and the LOS must be determined. Note that in order to separate the prompt emission in the spectra and to obtain the density of the fully stripped helium, knowledge of the He^{+} density is required, which in turn requires an initial assumption on the He^{2+} density.

As such, any attempt to model the helium plume emission entails the solution of the continuity equation for the transport of He^{+} ions along the magnetic field lines. He^{+} ions in the plasma can be produced through charge exchange of fully stripped helium with deuterium and through electron recombination of He^{2+}. The helium plume ions are produced through the first reaction and the source of hydrogen-like plume ions is given by:

$$S_{He^{+}} = \sum_{i=1}^{4}\sum_{n=1}^{2}\langle\sigma\upsilon\rangle_{i,n}^{CX,tot}n_{He^{2+}}n_b^{i,n}, \tag{4}$$

where the total rates for charge exchange reactions from He^{2+} to He^{+} ($\langle\sigma\upsilon\rangle_{i,n}^{CX,tot}$) have been used. The loss mechanism is the ionisation process due to electron and ion impact:

$$L_{He^{+}} = \frac{n_{He^{+}}}{\tau_{ion}}, \tag{5}$$

where τ_{ion} is the ionisation time. Electron impact ionisation is the most important process for ASDEX Upgrade relevant parameters and the only one that has been taken into account in this work. The complete set of atomic processes that contribute to the loss of helium plume ions also includes ion impact ionisation, which is relevant only at higher ion temperatures. Charge exchange with hydrogen-like ions is negligible and charge exchange with fully stripped helium is not considered as in practice no He^{+} ions are lost.

Assuming steady state conditions, i.e. $\frac{\partial n_{He^{+}}}{\partial t} = 0$, and that the plume ions are only allowed to move collisionessly along the magnetic field lines (along x) with a single velocity $\upsilon_{\|}$, then:

$$\upsilon_{\|}\frac{\partial n_{He^{+}}(x)}{\partial x} = \sum_{i=1}^{4}\sum_{n=1}^{2}\langle\sigma\upsilon\rangle_{i,n}^{CX,tot}(x)n_{He^{2+}}(x)n_b^{i,n}(x) - \frac{n_{He^{+}}(x)}{\tau_{ion}}, \tag{6}$$

where the source and loss terms can be identified on the right hand side. Perpendicular transport is ignored as it is negligible in comparison to the transport along the field lines. As the gyroradius of thermal helium is much smaller than the density and temperature gradient lengths in the plasma core, its effect on the ionisation probability is very small.

However, one should consider the Maxwellian velocity distribution of the source ions, and then the continuity equation for the distribution of the He^{+} ions $f(x, \upsilon_{\|})$ can be written as:

$$\upsilon_{\|}\frac{\partial f}{\partial x} = \sum_{i=1}^{4}\sum_{n=1}^{2}\langle\sigma\upsilon\rangle_{i,n}^{CX,tot}(x)n_{He^{2+}}(x)n_b^{i,n}(x)\frac{1}{\sqrt{\pi}\upsilon_{th}} \times \exp\left(-\frac{(\upsilon_{\|}-\upsilon_{rot})^2}{\upsilon_{th}^2}\right) - \frac{f}{\tau_{ion}}. \tag{7}$$

Once the density of the He^{+} along the magnetic field lines $n_{He^{+}}(x)$ is known, the density of the He^{+} along each diagnostic LOS can be evaluated. Subsequently, the plume emission for each LOS can be derived from (3). However, to enable the complete interpretation of the helium charge exchange spectra and then the derivation of accurate T_i, v_ϕ and $n_{He^{2+}}$ profiles, detailed information on the space and velocity distribution of the plume ions is needed, i.e. the correct $\upsilon_{\|}$ in the above equations is needed. This is discussed in the following section.

Note that the plume effect is significant for He^{2+}, but negligible for the visible CXRS lines of other impurities such as B^{5+}, C^{6+} and Li^{3+}. The plume contribution to the charge exchange spectra of helium and carbon can be compared by

looking at the ionisation and excitation rates of He^+ and C^{5+}, for typical plasma parameters. For example, for $n_e = 8 \times 10^{19}\,m^{-3}$ and $T_e = T_i = 3\,keV$, the electron impact ionisation rates for helium are about 23 times higher than those of carbon. Defining the ionisation length as $\lambda_{ion} = \upsilon_{th}(T_i) \cdot n_e^{-1} \cdot q_{ion,e}(T_e, n_e)^{-1}$, where $\upsilon_{th}(T_i) = \sqrt{(2 \cdot T_i)/m_i}$ is the group thermal velocity of the ions, the distance that the helium plume ions travel before being ionised is approximately 0.07 times the distance that the carbon plume ions travel. In other words, carbon plume ions have the chance to spread along the field line, while the helium plume ions tends to be centred near the source and have a higher chance to be observed, if excited by electron impact. This also means that for the same source rate there are more carbon than helium plume ions. However, the dominant effect is that the electron impact excitation rates for He^+ are about 200 times higher than those for C^{5+}, while the photon emission of the latter is taking place mostly unseen.

3. A model for the helium plume emission implemented at ASDEX Upgrade

As the helium plume emission is 'in-phase' with the prompt, or direct active charge exchange signal, it always contributes to the helium charge exchange spectra when there is an active signal, in other words when the neutral beam is on. It cannot be subtracted using techniques such as beam modulation. For this reason, the helium plume emission has to be modelled in order to evaluate the He^{2+} charge exchange spectra correctly.

One could consider the ratio of plume to prompt emission for each LOS as a first approximation to deduce correct $n_{He^{2+}}$ profiles. The He^{2+} density at a certain location in the plasma calculated without taking into account the helium plume effect can be corrected in the following way:

$$n_{He^{2+}}^{\text{plume-corrected}} = \frac{1}{1+R} n_{He^{2+}}^{\text{no correction}}, \tag{8}$$

where R is the ratio of plume to prompt emission intensities $R = I_{Plume}/I_{CX}$. An iterative scheme is, nevertheless, required to deduce the He^{2+} density, starting from an assumed input He^{2+} density profile and iterating the modelling until good agreement is found with the measured spectra (as will be discussed in section 4.2). However, for accurate interpretation of the spectra and to deduce correct T_i and v_ϕ profiles, more detailed information on the combined spatial and velocity distribution of the plume ions along the LOS is required.

At ASDEX Upgrade, a model for the helium plume emission has been developed that deals with this issue. It consists of the following steps:

(i) All of the background plasma profiles needed for the calculation are collected from routine ASDEX Upgrade diagnostics. The electron temperature and density profiles are obtained routinely from the Integrated Data Analysis procedure described in [12]. The ion temperature and rotation profiles cannot be correctly deduced from helium line before the plume emission is taken into account. They are, therefore, obtained from a charge exchange diagnostic that is measuring an impurity other than helium, for example boron or carbon. For these impurities the plume effect is negligible, as already discussed. An initial assumption for the He^{2+} density is needed and as an initial guess it is defined as $n_{He^{2+}} = c \cdot n_e$, where c is an initial assumption for the helium concentration in the plasma, or calculated from the measured charge exchange intensity, without taking into account the plume.

(ii) The diagnostic LOS geometry and the neutral beam geometry are used. The plasma equilibrium is used to trace the magnetic field lines through the plasma, so that the distribution of the plume ions along the field lines can be determined. For each point along the LOS a magnetic field line is traced around the torus.

(iii) The distribution of the neutral particles in the beam volume is calculated. To this end, the forward-modelling code FIDASIM, a Monte Carlo code that models the density of the beam and beam halo neutrals [13], can be used to calculate the neutral beam attenuation. Information on the neutral beam density can also be inferred from beam emission spectroscopy [14]. Alternatively, a simpler model of the neutral beam geometry and neutral attenuation, by means of a full collisional radiative model, can be used.

(iv) The He^+ ions that are born after charge exchange of He^{2+} ions with beam atoms are calculated along the magnetic field lines that cross the beam volume.

(v) These He^+ ions are followed along the magnetic field lines and their loss through a number of atomic processes, electron impact ionisation being the most important loss mechanism for ASDEX Upgrade relevant parameters, is evaluated. The modelling of the He^+ distribution along the field lines and in velocity space is discussed in section 3.1.

(vi) Some of the He^+ ions undergo electron impact excitation in the LOS of the diagnostic, and the plume photon flux and its wavelength distribution are derived using the appropriate photon emission coefficients.

The emission along each LOS is integrated, providing the total plume emission observed for each LOS. All atomic data needed and used in this work are obtained from the ADAS database [11]. The excitation rates from ADAS were expanded up to 20 keV by running the GCR codes within ADAS, which were also used earlier to derive the original data [15].

3.1. Space-velocity distribution of helium plume ions

The transport of helium plume ions along the magnetic field lines is given by the continuity (transport) equation, assuming steady state conditions. The determination of the parallel velocity of the plume ions is non-trivial and has important repercussions for the determined plume emission. There are several approaches to determining $\upsilon_\parallel$. First, it can be assumed that all plume ions move with a single velocity equal to the

thermal velocity of the He^{2+} ions, an assumption followed in [6, 9]. Second, the plume ions can be assumed to be born with and maintain a Maxwellian distribution of velocities equal to that of the He^{2+} in that location, as was done in [3]. Furthermore, a Monte Carlo approach can be used to determine the density and velocity of the He^{+} ions along the magnetic field line.

With the first assumption, the plume ions move along the magnetic field line away from the birth location with a velocity $v_{\parallel} = v_{\mathrm{th}}$ in both the positive and negative directions. Due to ionisation losses, the plume ion density is assumed to attenuate exponentially along the magnetic field lines according to $n_{\mathrm{He}^{+}} = c(x)\exp\left(-\frac{x}{v_{\parallel}\tau_{\mathrm{ion}}}\right)$ where τ_{ion} is the ionisation time. The ionisation time depends on n_e and T_e which are constant on a magnetic flux surface, and hence is a constant of the magnetic field line. A similar assumption has been applied in [6], where an attenuation factor for the helium plume across the magnetic field line is defined.

However, the He^{2+} ions in the plasma have a Maxwellian velocity distribution, and it is far more realistic to assume that the He^{+} ions born from the charge exchange reactions retain the same velocity distribution. If one assumes that all plume ions have a single velocity, an error is inevitably introduced in the prediction of the helium plume emission. Particles with higher or lower velocities than the thermal velocity will be distributed differently along the field lines and, consequently, the probability that they are in the observation region when they are excited is different.

For the case with a Maxwellian velocity distribution, the solution to the continuity equation is again straightforward: the He^{+} ions, despite being born with a Maxwellian distribution of velocities, can no longer be described by a Maxwellian distribution once they are spread along the magnetic field lines. The factor $\exp\left(-\frac{\Delta x}{v_{\parallel}\tau_{\mathrm{ion}}}\right)$, where Δx is the displacement along the magnetic field line, 'distorts' the Maxwellian distribution. This factor depends, not only on the location on the magnetic field line (Δx), but also on the local plasma parameters, as the ionisation time is a function of the electron temperature and density of the flux surface in which the field line lies.

Non-Maxwellian effects arise because the plume particles are not equilibrated via collisions with the background ions (see also [16]), as the momentum exchange time is much larger than the ionisation time (almost 3 to 4 orders of magnitude larger in the plasma core). As a consequence, the faster particles in the original Maxwellian velocity distribution leave the observation volume, while the slower remain, leading to smaller apparent ion temperatures and rotations. An illustration of this phenomenon can be seen in figure 1, where the distribution of $n_{\mathrm{He}^{+}}$ along a magnetic field line is shown in the top plots, for a case with zero rotation and a case with a rotation of $150\,\mathrm{km\,s^{-1}}$. The distribution is calculated using the kinetic equation for the $n_{\mathrm{He}^{+}}$ ions. Assuming a tangential view to the magnetic field lines, the plume ions over three different ranges in x are summed together and their velocity distributions are shown in the bottom plots. If particles from far away are included (total distance 7 m, red lines), the velocity distribution is almost Gaussian. However, if the sum is over a much narrower range along the field line (~60 cm), as is the case in reality, a much narrower velocity distribution is obtained, meaning a 'colder' and 'slower' emission line.

To deal with this, a Monte Carlo approach has been used to describe the distribution of the plume ions along the magnetic field lines (also for the illustrations in figure 1). In this case, a large number of Monte Carlo particles starts at a certain location on the field line, for example the intersection of the central beam axis with the flux surface. Then each of these particles is randomly assigned a velocity from a Maxwellian velocity distribution corresponding to the temperature and velocity of the background plasma at the birth location. The particle is then followed along the magnetic field line until its ionisation. The particle travels the distance from its birth location to the ionisation location with a fixed parallel velocity. On its way it is assigned to all locations along the magnetic field line grid according to its time of presence and classified in a velocity grid. The resulting normalised distribution of Monte Carlo particles along the field line and in velocity space is convoluted with the plume ion source in order to provide the plume ion distribution. As such, the Monte Carlo modelling provides not only the spread of the plume ions, but also their velocities. In other words, the kinetic effects of the plume and an accurate description of the plume ions in velocity space are obtained.

In figure 2, the distribution of the He^{+} ions along the magnetic field line is illustrated. The He^{+} ions are born from charge exchange reactions between He^{2+} and a neutral beam with a Gaussian source profile. In this case, the half width at half maximum of the beam is equal to the decay length of the ionisation (for ions with v_{th}) divided by 7. A Mach number of $M = 0.2$ is selected for the mean parallel velocity in the positive x direction, so that the Maxwellian distribution is shifted with $v_{\mathrm{M}} = 0.2v_{\mathrm{th}}$. Three density distributions of the He^{+} ions along the magnetic field lines are shown: (a) the kinetic description, as described above, in green, (b) the distribution assuming two equally weighted populations with constant velocity $v = (M \pm 1)v_{\mathrm{th}}$ and (c) the distribution assuming two equally weighted populations with constant velocity $v = (M \pm 0.44)v_{\mathrm{th}}$, which results into the same maximum density as the kinetic description. The two populations moving in the positive and negative directions are shown with dashed lines.

Comparing the distributions of plume ions assuming single velocities with the kinetic description, one sees that the assumption of a constant velocity $v = (M \pm 1)v_{\mathrm{th}}$ (red line) leads to underestimation of the amount of plume ions in and close to the beam volume, which is where most of the plume emission comes from. The case with $v = (M \pm 0.44)v_{\mathrm{th}}$ (blue line), results in similar values as the kinetic description, nevertheless, the shape of the distribution is not the same, which will be problematic when one attempts to reproduce the spectral emission line. Also, with the Monte Carlo approach,

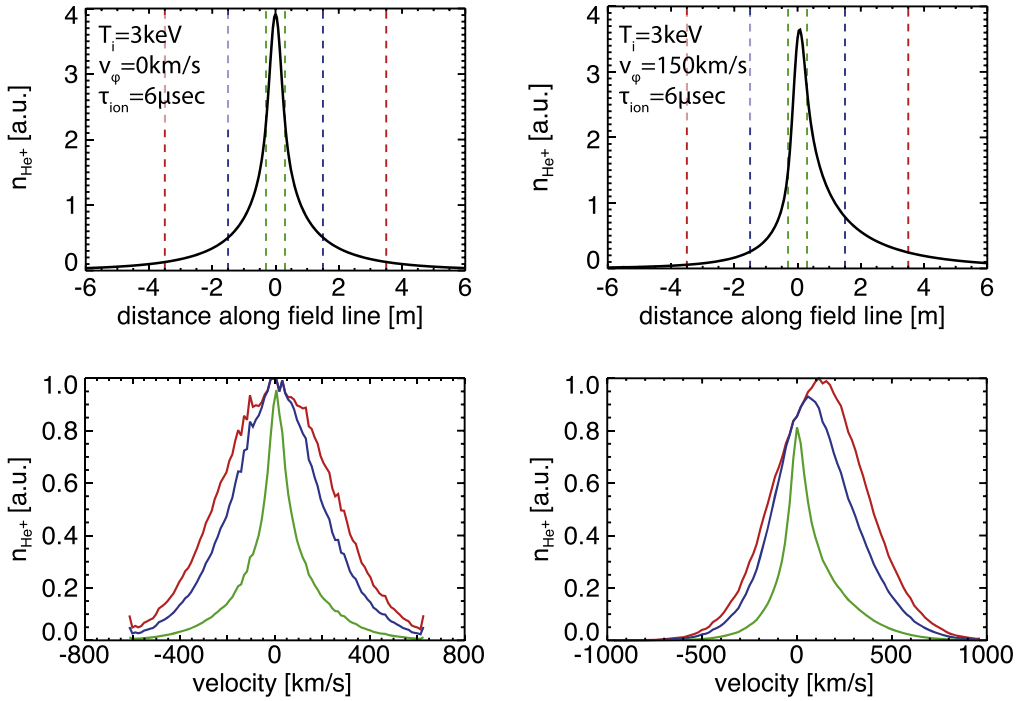

Figure 1. Distribution of plume ions along a magnetic field line (top plots) for zero rotation (left) or $v_\phi = 150\,\mathrm{km\,s^{-1}}$ (right). In the bottom, the corresponding velocity distributions of plume ions summed over the ranges indicated in the top plots (red, blue and green lines), normalised over the maximum value of the red curve.

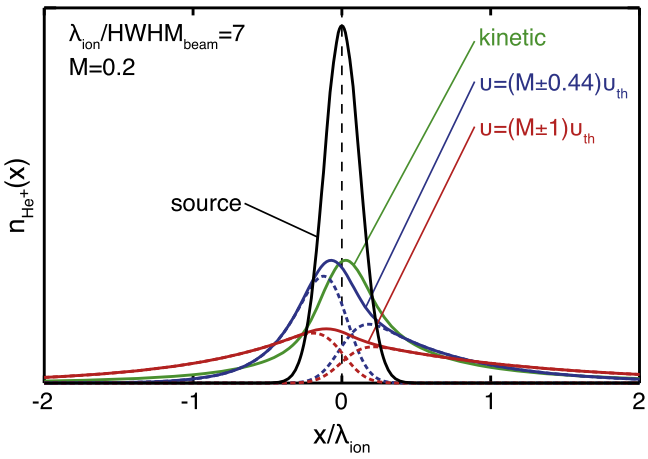

Figure 2. The distribution of He^+ ions along the magnetic field line for a Gaussian source profile (black), for two equally weighted populations with constant velocity of $(M \pm 1)\upsilon_{\mathrm{th}}$ (red) and $(M \pm 0.44)\upsilon_{\mathrm{th}}$ (blue). The distributions of the two populations moving in the positive and negative directions are shown with dashed lines. The kinetic description of the plume ion distribution is shown in green.

the distribution in real and velocity space is obtained, allowing for an accurate reconstruction of the plume spectral emission.

3.2. Dependencies of the helium plume

The helium plume emission is given by a complicated interplay between the diagnostic observation geometry, the magnetic equilibrium as well as the local plasma parameters including electron density, electron and ion temperature, plasma rotation, He^{2+} density and the neutral beam characteristics (beam voltage and halo). The dependence of the plume emission on each of these parameters has been examined in detail using the described Monte Carlo model. Here we summarise the most important parameters for the ASDEX Upgrade case.

The observation geometry of the diagnostic defines how much the helium plume emission pollutes the spectra. Diagnostic LOS that are parallel or almost parallel to the magnetic field lines, i.e. with toroidal observation geometry, will observe higher levels of plume emission than LOS viewing the neutral beam perpendicularly to the magnetic field lines, i.e. with purely poloidal observation geometry, assuming that the LOS are focussed to the axis of the neutral beam. Nevertheless, as the plume emission is localised close to the actual measurement location (in and close to the neutral beam volume), even purely poloidal observation geometries have to deal with a significant amount of plume emission in the spectra. Furthermore, the effect on the measured ion temperature and rotation will be different, as they measure even fewer of the plume ions with higher velocities. The plume intensity depends on the path of the LOS through the plume ion cloud. Looking at figure 3, the path of a poloidal LOS through the plume cloud is not negligible. The poloidal observation geometries are certainly much less hindered by the plume effect in comparison to predominantly toroidal views. Even so, the plume emission contributing to the spectra is not negligible and should be taken into account.

The plume emission depends on the electron density (see equation in section 2), as both the source and the loss of the plume ions depend on n_e, and so do the electron impact

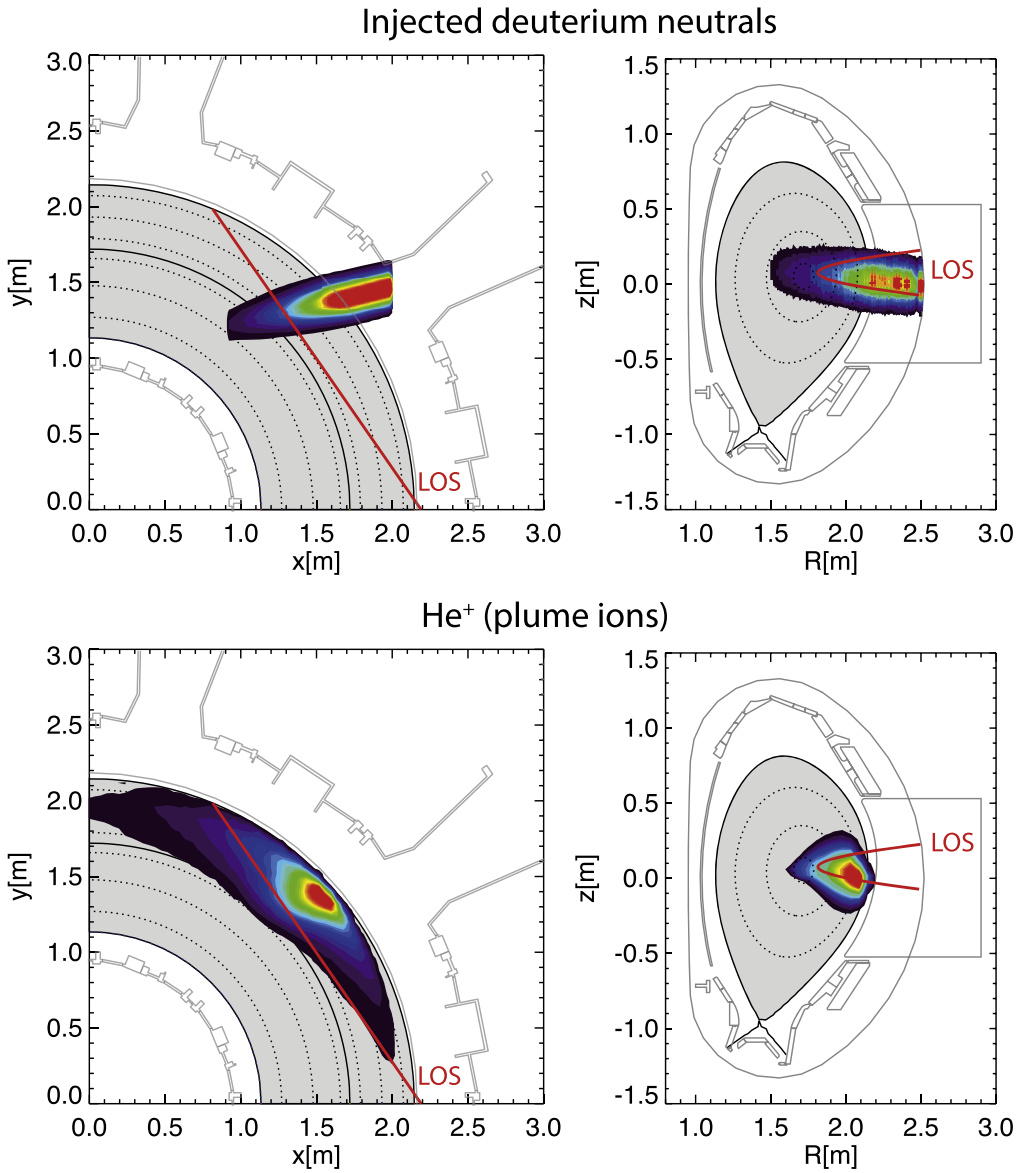

Figure 3. Top: the beam neutrals of NBI #3 injected into the plasma are shown in a top-down and a poloidal view of ASDEX Upgrade together with a LOS of the diagnostic, for #29083 at $t = 2.575$ s ($T_e(0) = 3.0$ keV, $n_e(0) = 6 \times 10^{19}$ m^{-3}, $T_i(0) = 2.5$ keV, $v_\varphi(0) = 95$ km s^{-1}). The intersection of the LOS with the beam injected neutrals shows where the measured signal from the charge exchange reactions between neutral deuterium and He^{2+} ions come from. The He^{+} ions are born in the volume of the neutral beam. In the bottom, the spatial distribution of these plume ions as they spread along the field lines is depicted. Note that the LOS intersects with this extended volume and, therefore, collects plume emission that originates in many different radial positions. For this figure, the full Monte Carlo model described here was used.

excitation and ionisation coefficients. Most importantly, as the correlation of the He^{2+} density profile with the electron density gradient is an important part of helium transport studies, it is interesting to investigate how big the mistake in the helium density and density gradient would be if the plume effect is ignored. The difference in the magnitude (which, for reference, is about a factor of almost 2 for the ASDEX Upgrade CXRS system) is the main factor. Also, the shape of the electron density profile can play an important role and lead to a significant difference between the gradient of the apparent helium density profile (calculated without taking the plume into account) and that of the real profile. For the ASDEX Upgrade system examined here, not taking into account the plume emission in the spectra can make the helium density profiles appear more hollow or more flat than they actually are. The difference is, however, usually within the uncertainty of the calculated gradient. Significant difference can, nevertheless, be observed in some cases, for example with very peaked or very flat electron density profiles. It is, therefore, important to examine the helium emission in detail for the given diagnostic system before drawing conclusions on the helium density profile peaking.

The concentration of He^{2+} in the plasma is not expected to alter the expected plume-to-prompt intensity ratio, as both the plume and prompt emissions will scale together in the same way. However, the shape of the He^{2+} density profile

(flat, hollow or peaked) plays an important role in the plume emission that is observed at each radial location. For toroidal LOS and a radially constant electron density profile, hollow He^{2+} density profiles would appear less hollow and flat He^{2+} density profiles would appear peaked. Additionally, the effect on the apparent helium density profile depends also on the shape of the electron density profile in comparison to that of fully stripped helium. It is, therefore, clear that the helium plume effect should be taken into account when evaluating helium density profiles and it is not simple to estimate the effect of the plume on the gradient without a proper calculation.

The plasma rotation influences the spread of the plume ion cloud along the magnetic field (see figure 1). Therefore, it strongly influences, indirectly, the probability that they are excited to the $n = 4$ state while still in the region of the LOS. The toroidal rotation affects the distribution of the helium plume ions along the magnetic field lines and along the LOS. Considering the plasma rotation is important for correctly reproducing the spectra and hence deriving correct ion temperature and rotation profiles from the helium spectra.

Furthermore, the charge exchange rates are lower for lower beam energy (for energies below the maximum in the rates). The partial charge exchange rates for the HeII $n = 4 - 3$ transition, however, fall more rapidly with the decrease in beam energy than the total charge exchange rates do. Consequently, as mentioned also in [6], the plume-to-prompt intensity ratio will be higher for lower beam energies. The voltage reduction affects the intensity of the prompt emission more strongly than that of the plume emission.

Finally, taking into account the neutral beam halo is very important for determining correct helium density profiles as it plays an important role in interpreting the prompt signal, but it is almost unimportant for the plume analysis. The thermal charge exchange is not sensitively influencing the total charge exchange rates, but it does influence the charge exchange rates into $n = 4$ and thus the charge exchange photon emission. Nevertheless, in this work, the beam halo is always taken into account.

4. Model benchmarking against experimental measurements

4.1. Derivation of helium density profiles using different observation geometries

The ASDEX Upgrade plasma discharge #29083 was specifically designed to benchmark the helium plume model presented here. The time traces of the most relevant plasma parameters during the discharge are shown in figure 4. In this discharge, the helium spectra were measured using the high étendue spectrometer described in [10]. The spectrometer was connected to two optical heads: one with predominantly toroidal LOS [17] and one with more poloidal LOS [13], both focussed on neutral beam source #3 (see figure 5). The plume-to-prompt intensity ratio is expected to be different for

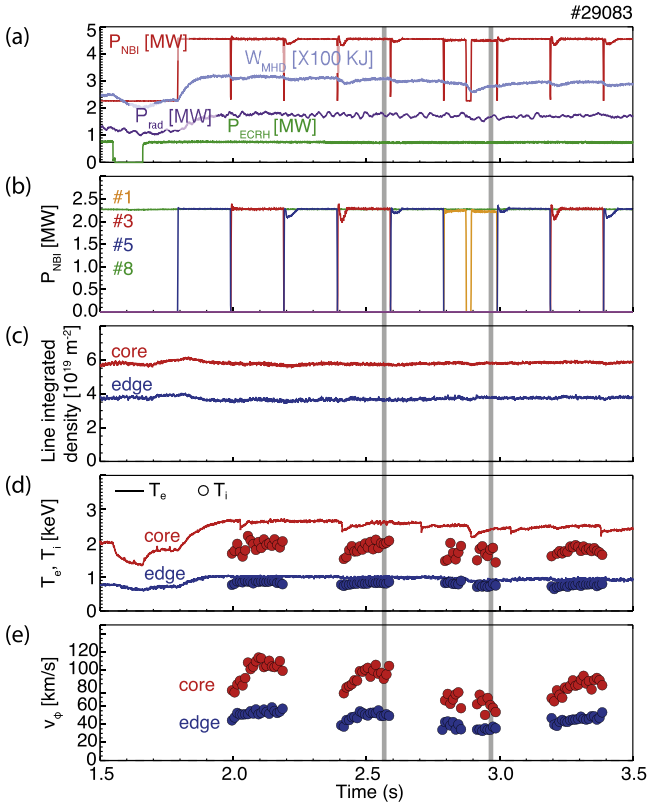

Figure 4. Time traces of the relevant parameters for discharge #29083: (a) injected NBI (red) and ECRH (green) power, radiated power (purple) and plasma stored energy (cyan), (b) details of the NBI replacement scheme, (c) line integrated electron density, (d) core ($\rho_{pol} \sim 0.2$) and edge ($\rho_{pol} \sim 0.8$) electron and ion temperature (lines and dots, respectively) and (e) toroidal rotation.

these two observation geometries, as their paths through the plume ion cloud are different, while the path lengths through the beam are similar.

The experimental discharge was planned to have stable plasma conditions and a very specific neutral beam injection scheme. The neutral beam source (#3) on which the helium and boron charge exchange measurements were performed was modulated such that the passive emission could be subtracted using the off-beam frames. The input power was kept constant by supplementing #3 with a source (#5) on the other side of the torus. It should be noted here that no plume ions originating at sources injected at the other side of the torus (namely sources #5–8) are expected to reach the spectrometer LOS. As an additional check, NBI source #3 was replaced by NBI source #1, for several phases of the plasma discharge. NBI #1 (also shown in figure 5) is more radial than NBI #3 and is situated below the toroidal LOS, hence less active emission from this source will be seen by the LOS and the ratio of plume to prompt signal will be different.

In the left plot of figure 6, the He^{2+} density profiles derived without taking into account the plume effect are shown for both sets of LOS. It is observed that the experimental density profiles measured by the poloidal and the toroidal LOS do not agree. This is expected as the LOS have

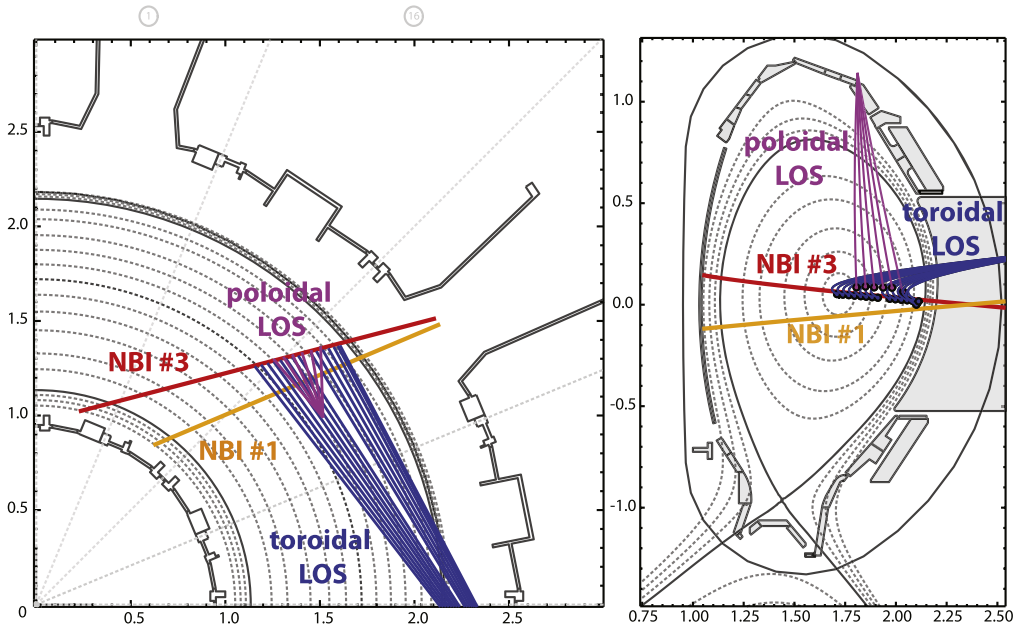

Figure 5. Top down and poloidal view of ASDEX Upgrade, with the geometry of the two sets of LOS and the two beam sources used in the experiment.

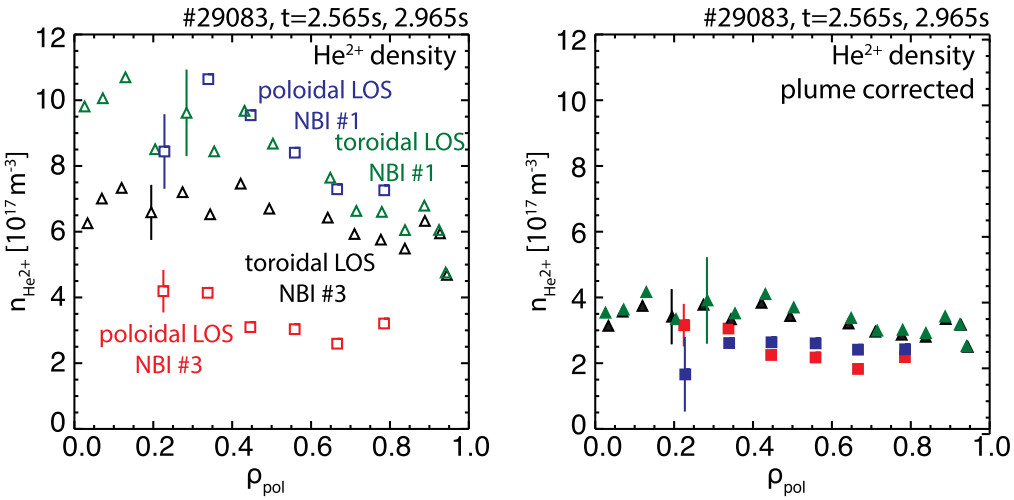

Figure 6. He^{2+} density profiles obtained from CX measurements for the ASDEX Upgrade discharge #29083 at 2.565 s (NBI #3 on) and at 2.975 s (NBI #1 on) without the plume effect taken into account (open symbols) and the corrected profiles after the plume effect has been modelled (filled symbols), for the toroidal and poloidal viewing geometry. Squares correspond to measurements with the poloidal LOS, while triangles correspond to the toroidal LOS. Red and black symbols correspond to measurements on NBI #3, blue and green symbols to NBI #1.

different geometries in relation to the magnetic field lines and the neutral beam and are therefore affected by the plume differently. The plume-to-prompt ratio for the toroidal LOS when NBI #3 is on is higher than the corresponding ratio for the poloidal LOS, as the path of the poloidal LOS through the plume cloud is smaller than for the toroidal ones (see also figure 7). In figure 8, the predicted prompt and plume emissions collected along a LOS are compared. The plume emission collected from a poloidal LOS is more localised and originates from the same volume as the prompt emission. The toroidal LOS, however, traverses a longer path through the plume and, therefore, plume emission is collected from an extended region.

Furthermore, the apparent helium density profiles measured on NBI #3 and NBI #1 are also different, despite the fact that the plasma parameters are very similar. The toroidal LOS are above the centre of NBI #1 and only view the edge of this source. As such, the prompt CX signal is lower by approximately a factor of 3 in the core. However, they still measure plume ions produced by NBI #1 which have followed the magnetic field lines into the LOS. In this case, the plume-to-prompt ratio in the core is almost a factor of 2 higher than for NBI #3. The poloidal LOS on the other hand barely intersect NBI #1 and measure almost exclusively the plume originating from NBI #1. The calculated plume-to-prompt ratio is indeed approximately 10 times higher in

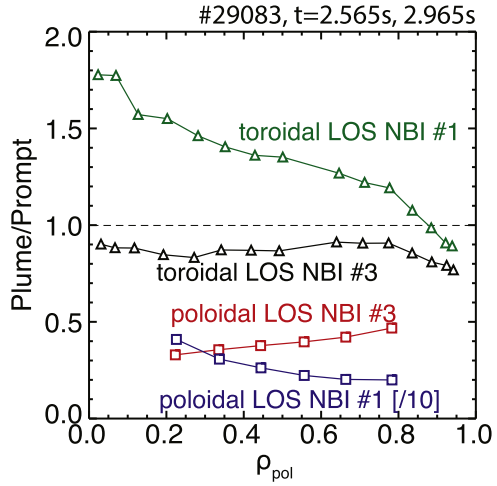

Figure 7. The plume-to-prompt intensity ratios calculated for the helium density measurements shown in figure 6. The values for the poloidal LOS looking on NBI #1 are divided by a factor of 10.

comparison to the ratio for the NBI #3 time point (shown divided by 10 in figure 7).

In the right plot of figure 6, the He^{2+} density profiles corrected with the plume emission model presented here are shown. The corrected densities are obtained by multiplying the densities in the left plot with a factor of $1/(1 + R)$, where R is the ratio of plume emission signal integrated along each LOS to the active CX signal, shown in figure 7, calculated using the full Monte-Carlo model. The corrected density profiles from the toroidal and the poloidal LOS are now in much better agreement, within the experimental uncertainties (note the error bars in the right plot in figure 6). The uncertainties on the impurity density profiles include the uncertainty of the measured intensity (intensity calibration) and the fitting of the spectra, as well as the uncertainties on the calculation of the neutral beam attenuation. The model also successfully reproduces the same impurity density profiles when evaluating the data from the #1 phase. Part of the remaining discrepancies can be attributed to intensity calibration uncertainties between the two optical heads. The ultimate test of the plume model is whether the line shape of the spectral plume emission can be predicted as well as correctly reproducing the T_i and v_ϕ profiles.

4.2. Modelling of the charge exchange spectrum including the plume emission component

The model for the helium plume emission described here provides not only a spatial distribution of the plume ions, but complete information about the distribution function of He^+ at each position in the plasma. It is, therefore, possible to reconstruct the plume emission spectral line.

The measured helium spectra without the passive emission, shown in green in figure 9, have a non-Gaussian shape. They consist of the prompt and the plume emission, which have different shapes: the prompt emission line has a Gaussian shape, while the spectral radiance of the plume emission can only be calculated after the distribution function of the plume ions is modelled. An additional passive contribution from the plasma edge, driven mainly by electron impact excitation of He^+ and by charge exchange of He^{2+} with thermal neutrals, complicates the analysis. For this reason, all investigations here have been performed with beam modulation in order to unambiguously remove the passive emission line. The total subtracted emission in the case presented here, is approximately half of the sum of the active and plume emissions. However, considerable care has to be taken when the neutral beam modulation technique is applied, so that the plasma conditions remain as constant as possible across the on- and off-beam frames. For this reason, the neutral beam on which the He CX spectra are measured is replaced by a neutral beam at the other side of the torus (see section 4.1).

As already discussed, it has been observed at ASDEX Upgrade, where charge exchange measurements on more than one impurity are routinely performed, that the ion temperature and rotation profiles derived from the HeII line differ from those measured on the BV (transition $n = 7 - 6$ at 494.467 nm) or CVI (transition $n = 8 - 7$ at 529.059 nm) lines if the plume emission line is not taken into account. Assuming that both the passive emission line and the plume emission line are correctly subtracted from the measured spectra, the remaining spectral shape, which is the isolated active charge exchange emission line, should yield ion temperature and rotation profiles that compare well with the boron or carbon measurements. The passive emission line is removed by means of subtracting passive frames during which the neutral beam is switched off, while the plume emission line shape is modelled.

The helium plume model provides the active (prompt) line and the plume emission lines, the sum of which can be compared with the measurements. The prompt emission line for each measurement location is represented by a single Gaussian shape, with a line shift $\Delta\lambda$ and a line width σ:

$$\Delta\lambda = \frac{v_{\mathrm{rot}}^{\mathrm{B}}\cos\gamma}{c}\lambda_0,\ \sigma = \sqrt{\frac{T_i^{\mathrm{B}}k_B}{mc^2}}\lambda_0, \tag{9}$$

where λ_0 is the natural wavelength (468.571 nm) and γ is the angle between the LOS and the toroidal direction. The superscript B denotes that boron measurements are used for the T_i and v_ϕ values at this location. The normalised Gaussian is multiplied with the total charge exchange radiance from equation (2) to obtain the spectral radiance.

The plume emission line, on the other hand, can not be described by a single Gaussian, due to the non-Maxwellian effects described in section 3. Additionally, the emission comes from many locations along the LOS, which are characterised by different T_i and v_ϕ values. The spectral radiance of the plume is given by:

$$\Phi_\lambda^{\mathrm{Plume}} = \frac{1}{4\pi}\int n_e(l)\,Q_{\mathrm{exc}}^{e}(l)\iint f_{\mathrm{He}^+}(l,\,v_\parallel,\,v_\perp) \times \delta\left[\lambda - \lambda_0\left(1 + \frac{v_\parallel}{c}\cos\gamma + \frac{v_\perp}{c}\sin\gamma\right)\right]\mathrm{d}v_\parallel\mathrm{d}v_\perp\,\mathrm{d}l, \tag{10}$$

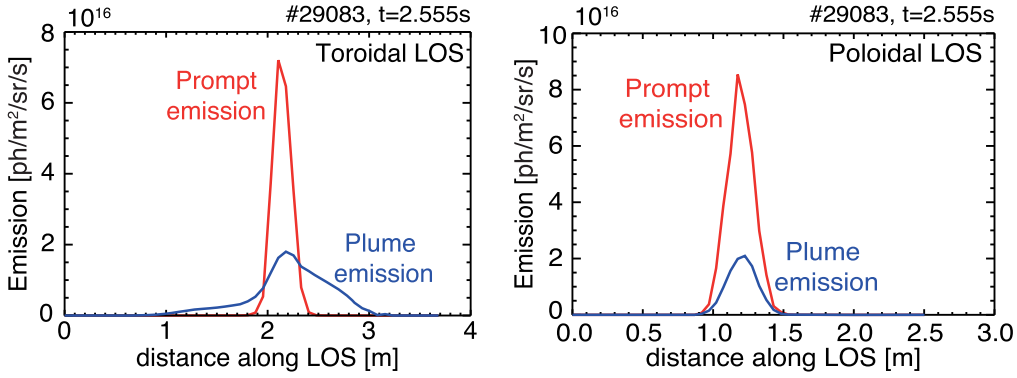

Figure 8. Plume and prompt emission along a toroidal and a poloidal LOS.

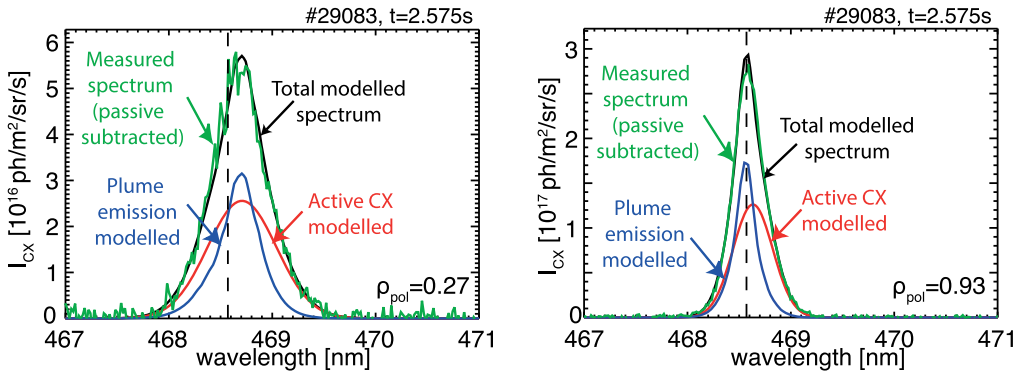

Figure 9. Reconstruction of helium charge exchange spectra for the toroidal viewing geometry, for discharge #29083, $t = 2.575$ s using the Monte Carlo method, for a core (left) and an edge LOS (right). Very good agreement is found between the sum of the reconstructed prompt and plume emission lines and the measured spectra, from which the passive emission has been subtracted.

where l gives the coordinate along the LOS, γ is the angle between LOS and the magnetic field line, $v_{\parallel}$ is the velocity parallel to the magnetic field $\vec{B}$ and $v_{\perp}$ is perpendicular to $\vec{B}$ in the plane defined by $\vec{B}$ and the direction of the LOS. As discussed, the helium plume ions are described by the distribution function $f_{He^+}(l, \vec{v})$ obtained by the Monte Carlo simulation which allows the reconstruction of the plume spectrum.

To extract accurate He^{2+} density profiles, the modelling of the helium plume line and the comparison of the modelled emission lines with the spectra has to be iterated. As already described in section 3.2, the plume emission depends on the shape of the He^{2+} density profile. Since this is an input to the modelling, comparison of the output modelled emission lines with the spectra is required and more iterations might be necessary. In simple words, an assumed He^{2+} density profile is used as input to the model: either the He^{2+} densities calculated ignoring the contribution of the plume or He^{2+} density profiles that follow the shape of the electron density profile can be used. The plume and prompt emission lines are reconstructed and compared to the measured spectra for all the LOS covering the plasma. A scaling factor is applied to the modelled emission lines to match the measurement, same for both emission lines, but possibly different between the different LOS. If the normalised residuals between the modelled and the measured spectrum are not satisfactory, the model is iterated once more, taking into account the scaling factors, which leads to a modification of the He^{2+} density profile as input to the plume model. The process can be repeated as many times as required to minimise the difference between the modelled and the measured spectrum. Good agreement is typically found within two to three iterations, within the error bars of the measured spectrum and the He^{2+} density profiles.

In figure 9, the reconstructed plume and prompt emission spectra are shown for a core and an edge LOS, in blue and red respectively. Their sum is compared to the measured spectra, from which the passive emission has been subtracted, using the passive spectra obtained right after the neutral beam is switched off. Very good agreement is found between the modelled and measured spectra.

In figure 10, measured ion temperature and rotation profiles of boron and helium are shown. The helium spectra, before being treated for the plume emission, fitted with a single Gaussian (passive subtracted using beam modulation) are shown in red. In blue, the profiles obtained from boron measurements and used as input to the modelling, are plotted. Additionally, the modelled plume emission line is subtracted from the helium spectra, which are subsequently fitted with a Gaussian, resulting in the profiles shown in magenta. Very good agreement is found with the boron measurements. Part of the remaining discrepancies are attributed to the method of the passive emission line subtraction. Ultimately this means that the plume model describes the involved physics to a high degree of accuracy, because not only the relative size of plume to prompt emission is described, but also the

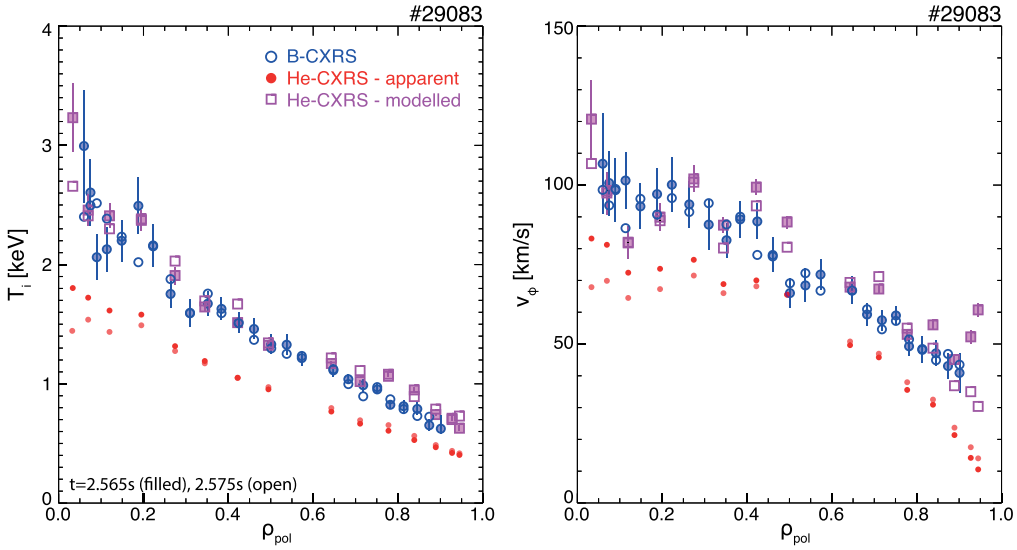

Figure 10. Reconstructed ion temperature and rotation profiles for the toroidal viewing geometry, for discharge #29083, at $t = 2.565$ s with filled symbols and at $t = 2.575$ s with open symbols (error bars shown only for the first time point). The profiles derived from boron measurements are shown in blue and the ones derived from helium measurements, without correcting for the plume are shown in red (apparent). The profiles derived from helium measurements after correcting for the plume are shown in magenta (modelled).

distribution of the plume in velocity space is matched. Thus, the observed differences in the He^{2+} density encountered in figure 6 are probably given by uncertainties in the intensity calibrations rather than by the plume model.

The final result of the model is subjected to the uncertainties of the input parameters and the diagnostic measurements. The measurement locations of the CXRS system are well characterised (radial resolution on the order of ± 1.5 cm). The absolute intensity calibration of the system, which is particularly important for the derivation of impurity densities, is associated with an error of 10%–15%. Furthermore, the uncertainties on the input plasma profiles (n_e, T_e, T_i, v_ϕ) also contribute to the modelling uncertainty. However, the uncertainties on the atomic data are not explicitly known. Finally, the magnetic equilibrium reconstruction, on which the tracing of the field lines relies, becomes increasingly less accurate the further into the plasma core. Even with these uncertainties on the input parameters, the model manages to reproduce the shape of the measured helium charge exchange spectra within the measurement uncertainty, which in the case presented is smaller than 7%.

5. Summary and outlook

In this work, the plume effect has been confirmed to be a significant contribution in the helium charge exchange spectra measured at ASDEX Upgrade. The plume emission contribution in the spectrum is complicated and depends on a number of plasma parameters, as well as on the diagnostic geometry, and needs to be treated appropriately. Accurate He^{2+} density profiles can be derived only if the plume emission is modelled and subtracted from the measured spectra.

Furthermore, it should be noted that the helium plume effect is important across the whole plasma radius, including the plasma edge. However, as the plume emission line has an apparent lower temperature and velocity than the active charge exchange line, it can easily be mixed with the passive emission line depending, of course, on the viewing geometry and edge plasma parameters. Furthermore, the helium plume effect can be minimised with the use of poloidal views, but still not avoided completely.

For the first time the non-Maxwellian features of the plume emission have been implemented in a model. This resulted in the breakthrough for the modelling of not only the helium plume-to-prompt ratio but also the modelling of the detailed charge exchange spectra including both the plume and prompt components.

This became possible through the consideration of the velocity space. This shows that the plume particles do not equilibrate with the background plasma, because the momentum exchange time is much longer than the ionisation time. Each plume particle, born with a Maxwellian velocity distribution, keeps their original parallel velocity along the magnetic field lines. The larger its parallel velocity the further the plume particle manages to travel. As such, the hot, fast particles streaming far away from the beam volume are not seen by the LOS, while the cold, slow plume ions which are centred near the beam volume, dominate the plume emission seen by the diagnostic. Finally, the ionisation time is short in comparison to the transition time around the torus and even the hot ions are lost before they reach again the observed volume. The modelling of this behaviour showed that the physics of the plume emission is captured correctly, as the experimental spectra can be reproduced.

The helium plume model is being developed further: starting from the measured helium charge exchange spectra and the derived T_i and v_ϕ values, which as described are affected by the helium plume emission, an iterative modelling process allows to converge to accurate T_i and v_ϕ profiles. This would allow for standalone charge exchange measurements based on

the HeII line, without the need for input from other impurity measurements for the modelling of the plume emission. However, in most cases the accuracy of the process is low.

Looking ahead at future fusion machines, for example ITER, the helium plume effect must be taken into account as charge exchange spectroscopy is expected to provide measurements of the helium 'ash'. Both the electron impact excitation rates and the electron impact ionisation rates will be lower at the higher electron temperatures of ITER, meaning in general lower plume emission intensities with increasing electron temperature. The higher electron densities mean shorter ionisation lengths for the He^{+} ions and more plume ions centred near the source. Yet the electron impact excitation rates drop with increasing density, resulting again into smaller contributions from the plume. In ITER conditions, however, ion impact ionisation and excitation will also become important. The LOS of the charge exchange diagnostic on ITER are designed to view the neutral beam polloidally with angles almost perpendicular to the magnetic field lines, in order to minimise the helium plume contribution [18]. Nevertheless, it is certain that the helium plume effect will be important for the thermal helium charge exchange measurements on ITER, and the magnitude of this effect can be estimated with the technique presented above.

To conclude, it should be stressed that the the helium plume is always present in the measured helium charge exchange spectra. It is of utmost importance to assess this emission at each fusion device, for each specific diagnostic geometry and plasma conditions. Furthermore, if ion temperature and rotation profiles are deduced from the helium charge exchange measurements, a spectral modelling of the helium plume is the most straightforward and reliable way.

Acknowledgments

This work has been carried out within the framework of the EUROfusion Consortium and has received funding from the Euratom research and training programme 2014–2018 under grant agreement No. 633053. The views and opinions expressed herein do not necessarily reflect those of the European Commission.

ORCID iDs

A Kappatou https://orcid.org/0000-0003-3341-1909
E Viezzer https://orcid.org/0000-0001-6419-6848

References

[1] 2007 Progress in the ITER physics basis *Nucl. Fusion* **47** S1–17
[2] Reiter D, Wolf G H and Kever H 1990 Burn condition, helium particle confinement and exhaust efficiency *Nucl. Fusion* **30** 2141
[3] Finkenthal D F 1994 The measurement of absolute helium ion density profiles on the DIII-D tokamak using charge exchange recombination spectroscopy *PhD Thesis* University of California, Berkeley
[4] Angioni C, Peeters A G, Pereverzev G V, Bottino A, Candy J, Dux R, Fable E, Hein T and Waltz R E 2009 Gyrokinetic simulations of impurity, He ash and α particle transport and consequences on ITER transport modelling *Nucl. Fusion* **49** 055013
[5] Kallenbach A and for the ASDEX Upgrade Team and the EUROfusion MST1 Team 2017 Overview of ASDEX upgrade results *Nucl. Fusion* **57** 102015
[6] Fonck R J, Darrow D S and Jaehnig K P 1984 Determination of plasma-ion velocity distribution via charge-exchange recombination spectroscopy *Phys. Rev.* A **29** 3288
[7] Gerstel U, Horton L, Summers H P, Von Hellermann M G and Wolle B 1997 Quantitative simulation of non-thermal charge-exchange spectra during helium neutral beam injection *Plasma Phys. Control. Fusion* **39** 737–56
[8] von Hellermann M G *et al* 2005 Complex spectra in fusion plasmas *Phys. Scr.* **T120** 19–29
[9] de Peña Hempel S 1997 Untersuchungen zum Transport leichter Verunreinigungen an ASDEX Upgrade *PhD Thesis* Technische Universität München
[10] Jaspers R J E *et al* 2012 A high etendue spectrometer suitable for core charge eXchange recombination spectroscopy on ITER *Rev. Sci. Instrum.* **83** 10D515
[11] Summers H P 2004 The ADAS User Manual, version 2.6 http://adas.ac.uk
[12] Fischer R, Fuchs C J, Kurzan B, Suttrop W, Wolfrum E and the ASDEX Upgrade Team 2017 Integrated data analysis of profile diagnostics at ASDEX Upgrade *Fusion Sci.Technol.* **58** 675–84
[13] Geiger B 2013 Fast-ion transport studies using FIDA spectroscopy at the ASDEX Upgrade tokamak *PhD Thesis* Ludwig-Maximilians-Universität München http://nbn-resolving.de/urn:nbn:de:bvb:19-153674
[14] Dux R, Geiger B, McDermott R M, Pütterich T, Viezzer E and the ASDEX Upgrade Team 2011 Impurity density determination using charge exchange and beam emission spectroscopy at ASDEX Upgrade *38th EPS Conf. on Plasma Physics (Strasbourg, France, 2011)* (http://ocs.ciemat.es/EPS2011PAP/pdf/P1.056.pdf)
[15] Summers H P, Dickson W J, O'Mullane M G, Badnell N R, Whiteford A D, Brooks D H, Lang J, Loch S D and Griffin D C 2006 Ionization state, excited populations and emission of impurities in dynamic finite density plasmas: I. The generalized collisional-radiative model for light elements *Plasma Phys. Control. Fusion* **48** 263–93
[16] Dnestrovskij A Y, Krupin V A, Klyuchnikov L A, Korobov K V, Naumenko N N, Nemmec A R and Tugarinov S N 2013 Underestimation of ion temperature in CXRS diagnostics of D-alpha spectra *Proc. 40th EPS Conf. on Plasma Physics (Espoo, Finland, 2013)* (http://ocs.ciemat.es/EPS2013PAP/pdf/P5.115.pdf)
[17] Viezzer E, Pütterich T, Dux R, McDermott R M and the ASDEX Upgrade Team 2012 High-resolution charge exchange measurements at ASDEX upgrade *Rev. Sci. Instrum.* **83** 103501
[18] von Hellermann M G, Jaspers R J E, Lotte P, Malaquias A and Tugarinov S 2002 Progress in charge exchange recombination spectroscopy (CXRS) and beam emission spectroscopy (BES) for ITER *Proc. 29th EPS Conf. Plasma Phys. Controlled Fusion (Montreux, 2002) Europhys. Conf. Abstracts* vol. 26B (http://epsppd.epfl.ch/Montreux/pdf/O5_07.pdf)